

Lattice parameter effects on the magnetic properties of the binary Ni/Bi alloy

*Mustafa Keskin and Numan Şarlı
Department of Physics, Erciyes University, 38039 Kayseri, Turkey

Abstract:

The influence of lattice parameters on the magnetic properties of the binary Nickel/Bismuth (Ni/Bi) alloy is investigated within the effective field theory. The temperature and applied field dependence of the magnetization of the Ni/Bi and its components (Ni, Bi1 and Bi2) are obtained. We find that the $T_c=2.31$ for the small lattice parameter ($ha/2$, $hc/2$ and $ra/2$), $T_c=1.14$ for the original lattice parameter (ha , hc and ra) and $T_c=0.59$ for the high lattice parameter ($2ha$, $2hc$ and $2ra$); hence, the critical temperature is inversely proportional with the lattice parameter. Similarly, hysteresis loop areas of the Ni/Bi alloy are also inversely proportional with the lattice parameters.

Key words: Binary Nickel/Bismuth alloy, magnetism, hysteresis, effective field theory

1. Introduction

Nickel (Ni) based alloys are advanced structural materials that are mainly used in aircraft engines but are also applied in the chemical, petrochemical and electrical industries [1, 2]. Binary Nickel-Bismuth (Ni/Bi) alloy is one of the Ni-based alloys which is used in ductility and grain-boundary (GB) segregation [3], intermetallic layers [4], hot dip galvanizing for steels to protect from atmospheric corrosions electrical contacts and magnetic layers [5], intermediate temperature embrittlement (ITE) [6], lead-free solders [7], lead-free solders [8] and superconductivity [9], etc. Because of these wide applications of the Ni/Bi alloys, these alloys have been already one of the actively studied subjects. For example, early experimental studies of Ni/Bi phase diagram were done by Portevin [10], Voss [11] and the detailed phase diagram of the Bi-Ni alloy was given by Nash [12]. Ely *et al.* [13] reported the first synthesis and characterization of Ni-Bi nanoparticles and nanowires via a very mild wet-chemical procedure. Yoshida *et al.* [14] studied the temperature dependent of magnetization as well as the SEM images and X-ray diffraction patterns. Piñeiro *et al.* [15] synthesized NiBi₃ polycrystals via a solid state method and also performed X-ray diffraction analysis. X-Ray, DSC and magnetic susceptibility measurements were performed with NiBi specimens in the interval from room temperature to 700 K by Vassilev and Lilova [16]. On the other hand, Jang *et al.* [17] studied the thermodynamic modelling of the Bi-Ni binary system was performed through the Thermo-calc® software package by using the CALPHAD method. Recently, ferromagnetic and paramagnetic properties of the binary Nickel/Bismuth alloy were studied within the effective field theory (EFT) by Keskin and Şarlı [18]. In particular, they studied the temperature dependence of Ni/Bi alloy and its components (Ni, Bi1 and Bi2). They have also studied the hysteresis loop behavior of Ni/Bi alloy and its components (Ni, Bi1 and Bi2) in detail.

In this paper, we investigate the lattice parameters effects on the magnetic properties of the Ni/Bi and its components within the EFT [19]. We obtain the temperature and applied field dependence of the magnetization of the Ni/Bi, namely hysteresis loops behavior, for the small lattice parameter,

and for the high lattice parameter than the original lattice parameter (h_a , h_c and r_a) of the Ni/Bi. We also present the behavior of coercivity fields of the alloy. We should also mention that since the lattice size varies with the temperature of the environment, the investigation of the effects of lattice parameters on the magnetic properties is very important for both technological applications and academic research. It is also worth mentioning that the EFT has been used to study magnetic properties of many physical systems such as cylindrical core and shell Ising nanowire [20], thin films [21], the equilibrium [22] and nonequilibrium [23, 24] phase transitions in Ising systems, Ising nanotube [25], Ising nanoparticles consisting of core and shell [26-28] and carbon diamond nanolattice [29], etc.

The organization of the rest of the paper is as follows. In section 2, the model and its formulation are given within the EFT. The numerical results and discussions are presented in Section 3 and Section 3 briefly contains the conclusion.

2. The model and formulation

In our very recent previous work [18], we investigated the ferromagnetic and paramagnetic properties of the binary Ni/Bi using the effective field theory (EFT). In this paper, we will investigate the influence of lattice parameters on the magnetic properties of the Ni/Bi and we will follow the same calculation procedures as in Ref. 18. But the main differences; we will change the original lattice parameters (h_a , h_c and r_a) as small lattice parameters ($h_a/2$, $h_c/2$ and $r_a/2$) and high lattice parameters ($2h_a$, $2h_c$ and $2r_a$).

We depict the Ni/Bi alloy with the rhombohedral Bi lattice ($r_a=4.7236 \text{ \AA}$ and $\alpha=57.35^\circ$) is surrounded by the hexagonal Ni lattice ($h_a=4.5330 \text{ \AA}$ and $h_c=11.7970 \text{ \AA}$) [30, 31] as shown in Fig.1 [18].

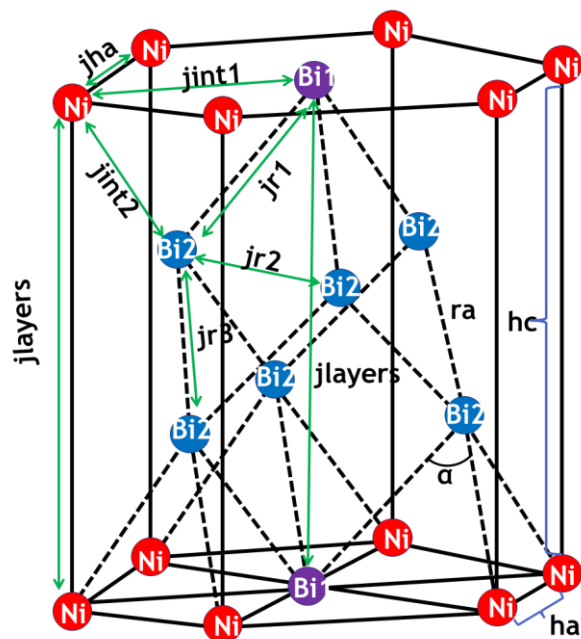


Figure 1. (Color online) Schematic depiction of the binary Nickel/Bismuth alloy (Ni/Bi) [18].

We assume that Ni and Bi components of the Ni/Bi alloy are Ising spin-1/2 particles for the calculations of the magnetic properties. According to lattice locations and nearest-neighbors, the Ni/Bi alloy has three different magnetizations that are Ni, Bi1 and Bi2. One notes that Bismuth atoms have two different magnetizations because of their lattice locations and their nearest-neighbors are different. The Hamiltonian of the Ni/Bi alloy can be written as,

$$\begin{aligned} \mathcal{H} = & -J_{ha} \sum_{\langle NiNi \rangle} S_{Ni}^z S_{Ni}^z - J_{r1} \sum_{\langle Bi1Bi2 \rangle} S_{Bi1}^z S_{Bi2}^z - J_{r2} \sum_{\langle Bi2Bi2 \rangle} S_{Bi2}^z S_{Bi2}^z - J_{r3} \sum_{\langle Bi2Bi2 \rangle} S_{Bi2}^z S_{Bi2}^z \\ & - J_{layers} \sum_{\langle NiNi \rangle} S_{Ni}^z S_{Ni}^z - J_{layers} \sum_{\langle Bi1Bi1 \rangle} S_{Bi1}^z S_{Bi1}^z - J_{int1} \sum_{\langle NiBi1 \rangle} S_{Ni}^z S_{Bi1}^z - J_{int2} \sum_{\langle NiBi2 \rangle} S_{Ni}^z S_{Bi2}^z \\ & - h \left(\sum_{Ni} S_{Ni}^z + \sum_{Bi1} S_{Bi1}^z + \sum_{Bi2} S_{Bi2}^z \right), \end{aligned} \quad (1)$$

where, $S^z = \pm 1$ is the Pauli spin operator. h is the external magnetic field. J_s are the exchange interaction between two nearest-neighbor atoms on the lattice of the Ni/Bi alloy, explained below and seen in Fig. 1. Moreover, they are designated as $J = k/nd$ [32, 33], k is a constant that defines the kind of magnetism (if $k=1 > 0$, the Ni/Bi alloy is ferromagnetic and if $k=-1 < 0$, the Ni/Bi alloy is antiferromagnetic), nd is the normalized lattice constant ($nd = d/1 \text{ \AA}$) [33], d is the distance between two nearest-neighbor atoms which is obtained by the real lattice constant of the Ni/Bi alloy. The real lattice constants, normalized lattice constants and exchange interactions of the Ni/Bi alloy are given by,

Original hexagonal lattice constants;

$$ha = 4.5330 \text{ \AA}, hc = 11.7970 \text{ \AA}.$$

Small hexagonal lattice constants;

$$ha/2 = 2.2665 \text{ \AA}, hc = 5.8985 \text{ \AA}.$$

High hexagonal lattice constants;

$$2ha = 9.066 \text{ \AA}, hc = 23.594 \text{ \AA}.$$

Original normalized hexagonal lattice constants;

$$nha = ha/1 \text{ \AA} = 4.5330, nhc = hc/1 \text{ \AA} = 11.7970.$$

Small normalized hexagonal lattice constants;

$$nha = ha/2 \text{ \AA} = 2.2665, nhc = hc/2 \text{ \AA} = 5.8985.$$

High normalized hexagonal lattice constants;

$$nha = 2ha/1 \text{ \AA} = 9.066, nhc = 2hc/1 \text{ \AA} = 23.594.$$

Original rhombohedral lattice constants;

$$ra = 4.7236 \text{ \AA} \text{ and } \alpha = 57.35^\circ.$$

Small rhombohedral lattice constants;

$$ra/2 = 2.3618 \text{ \AA} \text{ and } \alpha = 57.35^\circ.$$

High rhombohedral lattice constants;

$$2ra = 9.4472 \text{ \AA} \text{ and } \alpha = 57.35^\circ.$$

Original normalized rhombohedral lattice constants;

$$nra = ra/1 \text{ \AA} = 4.7236, \text{ and } \alpha = 57.35^\circ.$$

Small normalized rhombohedral lattice constants;

$$nra=ra/2 \text{ \AA} =2.3618, \text{ and } \alpha=57.35^{\circ}.$$

High normalized rhombohedral lattice constants;

$$nra=2ra/1 \text{ \AA} =9.4472, \text{ and } \alpha=57.35^{\circ}.$$

Original exchange interactions of the Ni/Bi alloy;

$$J_h=J_{r2}=J_{int1}=k/nha=0.2206,$$

$$J_{r1}=J_{r3}=J_{int2}=k/nra=0.2117,$$

$$J_{layers} (J_l)=k/nhc=0.0847.$$

Small exchange interactions of the Ni/Bi alloy;

$$2J_h=2J_{r2}=2J_{int1}=2k/nha=0.4412,$$

$$2J_{r1}=2J_{r3}=2J_{int2}=2k/nra=0.4234,$$

$$2J_{layers} (J_l)=2k/nhc=0.1694.$$

High exchange interactions of the Ni/Bi alloy;

$$J_h/2=J_{r2}/2=J_{int1}/2=k/2nha=0.1103,$$

$$J_{r1}/2=J_{r3}/2=J_{int2}/2=k/2nra=0.10585,$$

$$J_{layers} (J_l)/2=k/2nhc=0.04235.$$

Within the framework of the EFT [19], the magnetizations of the Ni, Bi1 and Bi2 (m_{Ni} , m_{Bi1} , and m_{Bi2}) components of the Ni/Bi alloy are given by

$$\begin{aligned} m_{Ni} &= \left[\cosh(J_{ha} \nabla) + m_{Ni} \sinh(J_{ha} \nabla) \right]^2 \left[\cosh(J_1 \nabla) + m_{Ni} \sinh(J_1 \nabla) \right]^1 \\ &\quad \left[\cosh(J_{int1} \nabla) + m_{Bi1} \sinh(J_{int1} \nabla) \right]^1 \left[\cosh(J_{int2} \nabla) + m_{Bi2} \sinh(J_{int2} \nabla) \right]^1 F_{s-1/2}(x) \Big|_{x=0}, \\ m_{Bi1} &= \left[\cosh(J_1 \nabla) + m_{Bi1} \sinh(J_1 \nabla) \right]^1 \left[\cosh(J_{r1} \nabla) + m_{Bi2} \sinh(J_{r1} \nabla) \right]^3 \left[\cosh(J_{int1} \nabla) + m_{Ni} \sinh(J_{int1} \nabla) \right]^6 F_{s-1/2}(x) \Big|_{x=0}, \\ m_{Bi2} &= \left[\cosh(J_{r2} \nabla) + m_{Bi2} \sinh(J_{r2} \nabla) \right]^2 \left[\cosh(J_{r3} \nabla) + m_{Bi2} \sinh(J_{r3} \nabla) \right]^2 \\ &\quad \left[\cosh(J_{r1} \nabla) + m_{Bi1} \sinh(J_{r1} \nabla) \right]^1 \left[\cosh(J_{int2} \nabla) + m_{Ni} \sinh(J_{int2} \nabla) \right]^2 F_{s-1/2}(x) \Big|_{x=0}, \end{aligned} \quad (2)$$

where, $\nabla = \partial / \partial x$ is the differential operator in the EFT and the function of $F_{s-1/2}(x)$ is defined by as follows for the spin-1/2 Ising particles.

$$F_{s-1/2}(x) = \tanh[\beta(x+h)] \quad (3)$$

where, $\beta=1/k_B T_A$, k_B denotes the Boltzmann's constant, T_A is the absolute temperature. In this paper we used the reduced temperature, namely $T=k_B T_A/J$ and the reduced applied field, i.e. $H=h/J$ in all calculations. The total magnetization of the Ni/Bi alloy (M_T) can be written by,

$$M_T = \frac{1}{20} [12m_{Ni} + 2m_{Bi1} + 6m_{Bi2}] \quad (4)$$

3. Results and Discussions

Fig.2 shows the temperature dependence of the magnetization of the Ni/Bi and its components (Ni, Bi1 and Bi2) for the small lattice parameter ($ha/2$, $hc/2$ and $ra/2$) and for the high lattice parameter ($2ha$, $2hc$ and $2ra$) than the original lattice parameter (ha , hc and ra) of the Ni/Bi. The critical temperature is obtained at $T_c=1.14$ for the original lattice parameter [18], at $T_c=2.31$ for the small lattice parameter and at $T_c=0.59$ for the high lattice parameter. Therefore, the T_c of the Ni/Bi and its components is inversely proportional with the lattice parameter. So, the T_c of the Ni/Bi and its components increases as the lattice parameter decreases or it decreases as the lattice parameters increase.

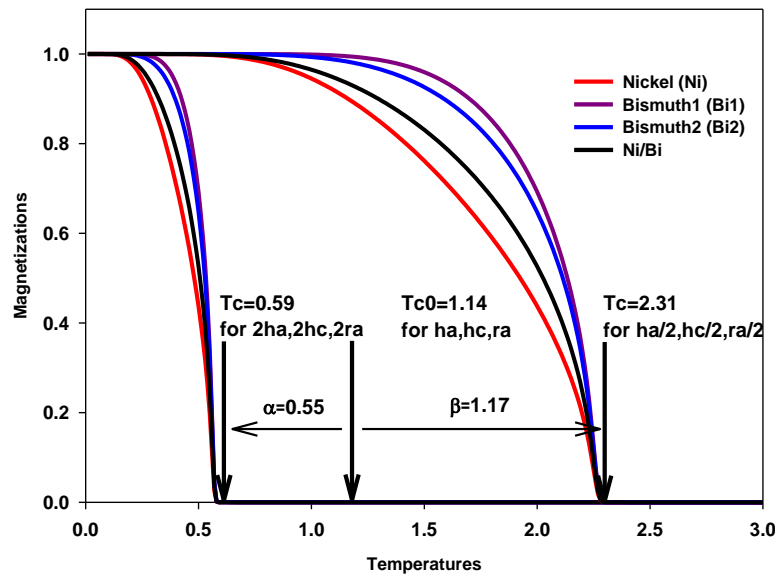


Figure. 2. (Color online) Lattice parameter effects on the behavior of thermal magnetizations of the Ni/Bi and its components.

Fig.3 shows the hysteresis loop behaviors of the Ni/Bi and its components (Ni, Bi1 and Bi2) for the small lattice parameter ($ha/2$, $hc/2$ and $ra/2$) than the original lattice parameter (ha , hc and ra) of the Ni/Bi. The coercive field (H_c) points are obtained as $H_c=0.89$, 0.56 , 0.06 and 0.000 at $T=0.5$, 1 , 2 and 3 , respectively for the small lattice parameter. On the other hand, $H_c=0.282$, 0.026 , 0.000 and 0.000 at $T=0.5$, 1 , 2 and 3 , respectively for the original lattice parameter. As we clearly see that the hysteresis loop areas or coercive field points of the Ni/Bi and its components are inversely proportional with the lattice parameter. So, they increase as the lattice parameters decrease according to the original lattice parameter.

Fig.4 shows the applied field dependence of the magnetization of the Ni/Bi and its components (Ni, Bi1 and Bi2) for the high lattice parameter ($2ha$, $2hc$ and $2ra$) than the original lattice parameter (ha , hc and ra) of the Ni/Bi. The hysteresis loop areas or coercive field points are obtained as $H_c=0.02$, 0.00 , 0.00 and 0.00 at $T=0.5$, 1 , 2 and 3 , respectively for the high lattice parameter. These values are small than those of the $H_c=0.282$, 0.026 , 0.000 and 0.000 at $T=0.5$, 1 , 2 and 3 , respectively for the original lattice parameter. So, they decrease as the lattice parameters increase according to the original lattice parameters.

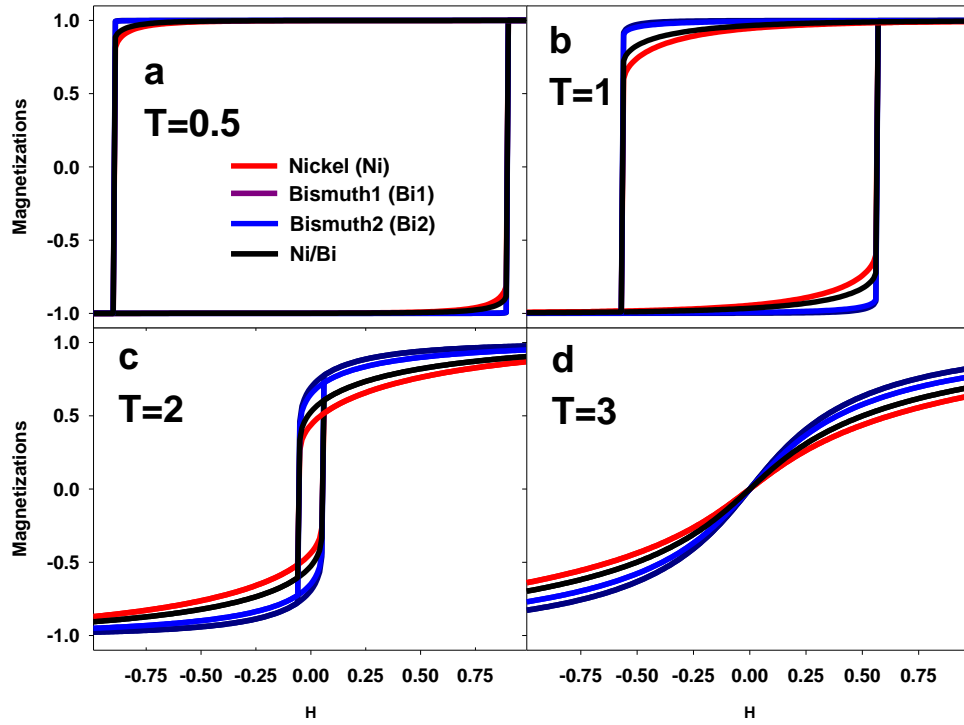


Figure 3. (Color online) Hysteresis behaviors of the Ni/Bi and its components for the small lattice parameter.

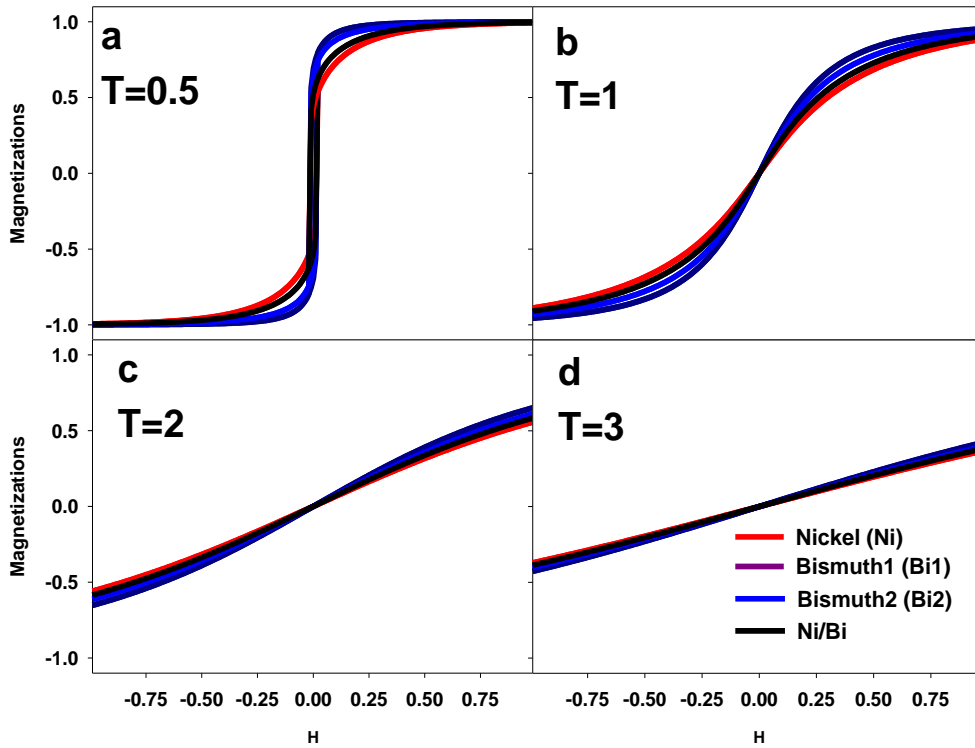


Figure 4. (Color online) Hysteresis behaviors of the Ni/Bi and its components for the high lattice parameter.

Fig.5 shows the lattice parameter dependence of the coercive field points of the Ni/Bi and its components (Ni, Bi1 and Bi2) for the small lattice parameter ($ha/2$, $hc/2$ and $ra/2$), for the high lattice parameter ($2ha$, $2hc$ and $2ra$) and for the original lattice parameter (ha , hc and ra) of the Ni/Bi. The H_c is inversely proportional with the lattice parameters, similar to the T_c . These results show us that when the original lattice parameters change, the magnetic properties change inversely proportional with the lattice parameters. From these results, we can suggest that it can be possible to obtain different magnetic properties of any system by tuning its lattice parameters.

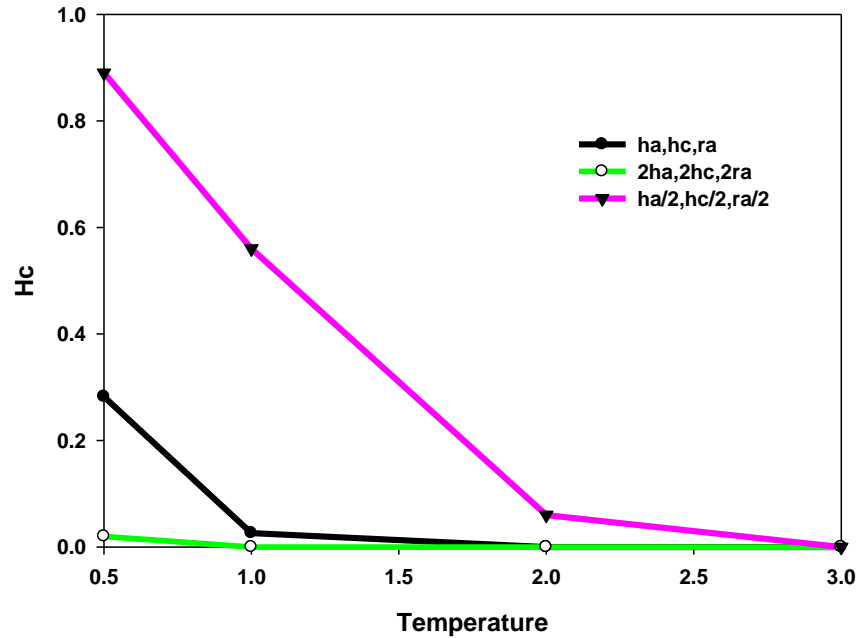


Figure 5. (Color online) Lattice parameter effects on the coercive field points of the Ni/Bi and its components

Conclusions

We investigated the temperature and applied field dependence of the magnetizations, namely hysteresis loop behaviors, of the Ni/Bi and its components for the small and high lattice parameter than the original lattice parameter. This investigation is very important for the technological applications, because of the lattice size varies with the temperature of the environment. We find that the T_c and H_c or hysteresis loop areas of the Ni/Bi and its components are inversely proportional with the lattice parameter. They increase when the lattice parameters decrease or they decrease when the lattice parameters increase. Similar behavior has been seen the trilayer Ising nanostructure with an ABA stacking sequence [28]. Hence, by tuning the lattice parameter, we can control the T_c and H_c of any system. Finally, we should also mention that hysteresis loop area is very important for technological applications. If the loop area is wide and big that corresponds hard magnet which can be useful for permanent magnets, magnetic recording and memory devices. On the other hand, if the loop area is thinner and narrower that corresponds soft magnets in which desirable for transformers and motor cores and AC applications. Moreover, the high coercivities correspond to the magnetically hard materials and low coercivities to the magnetically soft ones.

References

- [1] Neumeier S, Dinkel M, Pyczak F, Göken M. Nanoindentation and XRD investigations of single crystalline Ni–Ge brazed nickel-base superalloys PWA 1483 and René N5. *Mater Sci Eng. A* 2011;528:815–822.
- [2] Krupp U, Kane WM, Laird C, McMahon CJ. Brittle intergranular fracture of a Ni-base superalloy at high temperatures by dynamic embrittlement. *Mater Sci Eng A* 2004;387–389:409–413.
- [3] Marie N, Wolski K, Biscondi M, Grain boundary penetration of nickel by liquid bismuth as a film of nanometric thickness. *Scripta Mater* 2000;43:943-949.
- [4] Dybkov VI. Regularities Of reactive diffusion and phase formation In Ni–Bi, Ni–Zn, AND Co–Zn binary systems. *Powder Metal Met Ceram* 2001;40:7-8.
- [5] Fratesi R, Ruffini N, Malavolta M, Bellezze T. Contemporary use of Ni and Bi in hot-ip galvanizing. *Surf Coat Technol.* 2002;157:34–39.
- [6] Vassilev G, Gandova V, Docheva P. Comments and reconciliation of the Ni–Bi-system thermodynamic reassessments, *Cryst Res Technol* 2009;44:25-30.
- [7] Zheng L, Chellali R, Schlesiger R, Baither D, Schmitz G, Intermediate temperature embrittlement in high-purity Ni and binary Ni(Bi) alloy. *Scripta Mater* 2011;65:428-431.
- [8] Zheng L, Chellali MR, Schlesiger R, Meng Y, Baither D, Schmitz G, Non-equilibrium grain-boundary segregation of Bi in binary Ni(Bi) alloy. *Scripta Mater* 2013;68:825–828.
- [9] Siva V, Senapati K, Satpati B, Prusty S, Avasthi DK, Kanjilal D, Sahoo PK. Spontaneous formation of superconducting NiBi₃ phase in Ni-Bi bilayer film. *J Appl Phys* 2015;117:083902.
- [10] Portevin MA. The alloys of nickel and bismuth. *Rev Met* 1908;5:110-120.
- [11] Voss G. The nickel-bismuth system *Z. Anorg Chem* 1908;57:52-58.
- [12] Nash P. The Bi-Ni (bismuth-nickel) system. *Bull Alloy Phase Diagrams* 1985;6:345–347.
- [13] Ely TO, Thurston JH, Kumar A, Respaud M, Guo W, Weidenthaler C, Whitmire KH. Wet-Chemistry synthesis of Nickel-Bismuth bimetallic nanoparticles and nanowires. *Chem Mater* 2005;17:4750-4754.
- [14] Yoshida H, Shima T, Takahashi T, Kaneko T, Suzuki T, Kimura HM, Asami K, Inoue A, Magnetic properties of NiBi, *J Magn Magn Mater* 2002;239:5-7.
- [15] Piñeiro ELM, Herrera BLR, Escudero R, Bucio L. Possible coexistence of superconductivity and magnetism in intermetallic NiBi₃. *Solid State Commun* 2011;151:425–429.
- [16] Vassilev GP, Lilova KI, Notes on some supposed transitions of the phase NiBi. *Cryst Res Technol* 2007;42:237–240.
- [17] Jiang W, Gui MF, Bin LL. Thermodynamic optimization of Bi-Ni binary system. *Trans Nonferrous Met Soc China* 2011;21:139-145.
- [18] Keskin M, Şarlı N. Magnetic properties of the binary Nickel/Bismuth alloy. *J Magn Magn Mater* 2017;437:1-6.
- [19] Kaneyoshi T. Magnetizations of a transverse Ising nanowire. *J Magn Magn Mater* 2010;322:3410-3415.
- [20] Şarlı N, Keskin M. Two distinct magnetic susceptibility peaks and magnetic reversal events in a cylindrical core/shell spin-1 Ising nanowire. *Solid State Commun* 2012;152:354-359.
- [21] Wang CD, Ma RG. Force induced phase transition of honeycomb-structured ferroelectric thin film. *Physica A* 2013;392:3570-3577.
- [22] de Albuquerque D.F, Fittipaldi, IP, de Sousa JR. Absence of tricritical behavior of the random

- field Ising model in a honeycomb lattice. *J Magn Magn Mater* 2006;306: 92-97.
- [23] Ertas M, Deviren B, Keskin M. Nonequilibrium magnetic properties in a two-dimensional kinetic mixed Ising system within the effective-field theory and Glauber-type stochastic dynamics approach. *Phys Rev E* 2012;86:051110.
- [24] Shi X, Wei G. Effective-field and Monte Carlo studies of a kinetic Blume-Capel model. *Physica Scripta* 2014;89:075805.
- [25] Kocakaplan Y, Keskin M. Hysteresis and compensation behaviors of spin-3/2 cylindrical Ising nanotube system. *J Appl Phys* 2014;116:093904.
- [26] Kaneyoshi T. Phase diagrams of a nanoparticle described by the transverse Ising model. *Phys stat sol (b)* 2005;14:2938-2948.
- [27] Kantar E, Keskin M. Thermal and magnetic properties of ternary mixed Ising nanoparticles with core-shell structure: Effective-field theory approach. *J Magn Magn Mater* 2014;349:165-172.
- [28] Şarlı N, Akbudak S, Polat Y, Ellialtıođlu MR. Effective distance of a ferromagnetic trilayer Ising nanostructure with an ABA stacking sequence. *Physica A* 2015;43:194-200.
- [29] Şarlı N. Artificial magnetism in a carbon diamond nanolattice with the spin orientation effect. *Diamond Relat Mater* 2016;64:103-109.
- [30] Song TE, Wilde G, Peterlechner M. Morphology and aspect ratio of bismuth nanoparticles embedded in a zinc matrix. *Appl Phys Lett* 2014;105:241902.
- [31] Madelung O, Rössler U, Schulz M. (ed.) SpringerMaterials, Bismuth (Bi) lattice and structural parameters, thermal expansion, atomic weight and volume. Landolt-Börnstein - Group III Condensed Matter 41C (Non-Tetrahedrally Bonded Elements and Binary Compounds I) http://materials.springer.com/lb/docs/sm_lbs_978-3-540-31360-1_1179, 10.1007/10681727_1179 (Springer-Verlag Berlin Heidelberg © 1998).
- [32] Kittel C. Introduction to Solid State Physics, Seventh edition, John Wiley & Sons, Inc., New York 1999;333-378.
- [33] Şarlı N. Superconductor core effect of the body centered orthorhombic nanolattice structure. *J Supercond Nov Magn* 2015;28:2355–2363.